

Numerical modelling of the goaf: methodology and application

Samar S. Ahmed^{a*}, Marwan ALHeib^b, Yann Gunzburger^a, Vincent Renaud^b, Jack-Pierre Piguet^a

^a GeoRessources, Université de Lorraine, CNRS, Ecole des Mines de Nancy, Nancy, 54042, France

^b INERIS, Ecole des Mines de Nancy, Nancy, 54042, France

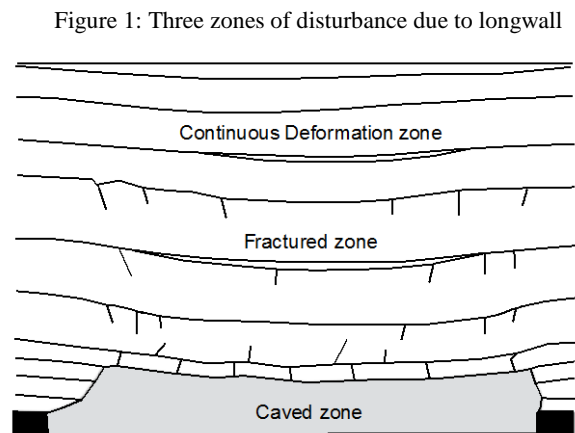
ABSTRACT

The mechanical behavior of the goaf is a critical issue that may affect the efficiency of longwall mining. Goaf numerical modelling as a continuous material is a challenge, especially because its large-scale mechanical properties are not precisely known. Many different values of the elastic modulus may be found in the literature to be used for representing the mechanical behavior of the goaf area. In the present study, the elastic numerical modelling is shown to be a useful tool for simulating the stress redistribution and displacement due to longwall mining, while taking into account the goaf geometry and its equivalent mechanical properties. The analysis is applied on the Provence coalmine, in the south of France, which had been in operation for more than 50 years, using the longwall mining method was used. A finite difference numerical model of the mine is constructed and two approaches are carried out in order to simulate the goaf area above the excavated panels where the panels have various length to width ratios. In the first approach, the caved zone and the fractured zone have different but homogeneous elastic modulus, both zones have elastic modulus lower than the unaffected host rock. In the second one, their elastic modulus varies linearly with the vertical distance above the panel, up to the elastic modulus of the host rock. In both cases with and without goaf, the subsidence at the ground surface is calculated and compared with in-situ measured values. Results show that attributing to the goaf area a low elastic modulus increases the vertical stress within the rib pillars as well as the subsidence at the surface. The elastic modulus for the direct roof above the panel after excavation has found to be $225 \leq E_{\text{immediate-roof}} \text{ (MPa)} \leq 180$ in order to satisfy the total convergence between the roof and the floor. Representing the goaf area as a material with linearly varying elastic modulus gives rational results in terms of convergence and ground surface subsidence.

KEYWORDS: Numerical modeling; goaf simulation; longwall mining; stress redistribution

1. INTRODUCTION

The longwall caving mining method is widely used in underground mines and fundamentally in coalmines that involve the exploitation of large rectangular panels. When the coal seam is extracted, three zones of disturbance due to longwall mining can be defined as shown in Figure 1 (Peng and Chaing, 1984). The caved zone corresponds to the immediate roof that totally collapses onto the floor. The fractured zone lies above the caved zone, where the rock strata are broken into blocks by essentially vertical and horizontal cracks associated with bed separation. The continuous deformation zone is only slightly influenced by the excavation. In the three zones, even if major cracks will appear, the rock mass behaves essentially as a continuous medium at large scale. In order to numerically simulate the whole mining process, their geometry and mechanical properties must first be determined. For example, Peng and Chaing (1984) proposed the thickness of the fractured zone to be 28 – 42 times the thickness (t) of the mined seam. Recently Shabanimashcool et al. (2012) found that the height of the caved zone is equal to $4t$.



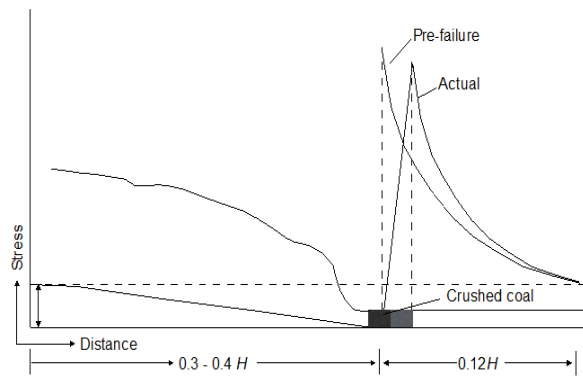
caving mining method (Peng and Chaing, 1984).

Assessment of the mechanical behavior of the goaf is very difficult due to the inaccessibility to the damaged area in the mine, as well as the heterogeneity of the goaf material. Much research has been undertaken on this topic, which is essential to determine the stress redistribution within the goaf area itself or onto the ribsides.

*Corresponding author – email: samar.ahmed@univ-lorraine.fr

Wilson (1980a) suggested that, after consolidation of the goaf, the vertical stress within the goaf increases linearly from zero at the ribsides to the pre-mining vertical stress at a distance from the ribsides equal to $0.3 - 0.4$ times H where H is the mining depth. Wilson (1982b) also suggested that the peak vertical stress on the ribsides (the “abutment pressure”) might be as high as six times the initial one. The generally accepted stress re-distribution developed by Wilson (1982b) is as shown in Figure 2. However, Wilson proposed a 2D estimation and he did not consider the effect of the third direction that may play an important role. Also, he did not refer to the material properties and its effect in stress redistribution.

Figure 2: Vertical stress distribution within the goaf and



the ribsides (Wilson, 1982b).

Sheory (1993) developed equations (1) and (2) to evaluate the elastic and bulk modulus (E and K) over the goaf span from his experience at Singareni coalfield in India:

$$E(x) = 600\left(\frac{x}{L}\right)^p \quad (1)$$

$$K_{goaf} = 0.0256 K_{hostrock} \quad (2)$$

where x is the distance from the ribsides, L is the half-span of the goaf measured perpendicularly to the work face and $p = 13\left(1 - \frac{x}{L}\right)^{0.29}$. Sheory’s model is very effective to estimate the elastic modulus along the panel span after excavation, but we could not estimate the modulus within the caved volume itself.

Salamon (1990) defined the stress strain relationship of the goaf material as:

$$\sigma = \frac{E_0 \varepsilon}{1 - (\varepsilon/\varepsilon_m)} \quad (3)$$

where, ε and σ are the vertical strain and stress respectively and E_0 is the initial elastic modulus of the

goaf material. ε_m is given by equation (4) using the buckling factor BF:

$$\varepsilon_m = \frac{BF - 1}{BF} \quad (4)$$

E_0 (MPa) can be calculated as a function of the compressive strength of the intact rock, σ_c , and the buckling factor (Pappas and Mark, 1993; Yavuz, 2004):

$$E_0 = \frac{10.39 \sigma_c^{1.042}}{BF^{7.7}} \quad (5)$$

Salamon’s model is valid for cave-in materials under hardening condition, and (non-elastic) behaviour. E_0 and ε_m must be detected firstly then the hardening table will be estimated by using equation (3).

In this research, the elastic mechanical model will be used in order to simulate numerically the goaf area above the excavation as well as to assess the mechanical consequences of longwall mining. Immediately after excavation, the goaf area will be substituted by less stiff material whose properties will be calibrated by the total convergence between the roof and floor of the panel and the ground surface subsidence.

2. CASE STUDY

The case study for this paper is the Provence coalmine, located in the south of France. It had been exploited between 1984 and 2004 using the longwall mining method, with a panel width of 200 m with various lengths, as shown in Figure 3.

Figure 3 represents the exploited panels between 1984 and 1994. The average thickness of the exploited coal seam is $t=2.5$ m, at a depth of 700 to 1100 m. The overburden is mainly composed of Fuvelian limestone and Begudo-Rognacian limestone and marl, as shown in Figure 4. The stiffness of the Rognacian layer is low compared with the adjacent Fuvelian layer because it contains a high percentage of marl and clayey limestone (Gaviglio, 1985). The initial mechanical properties of the different layer within the rockmass are given in Table 1 (Gaviglio et al., 1996).

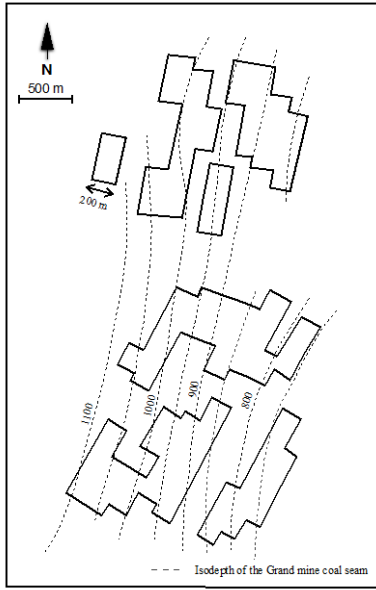


Figure 3: Excavated Panels in Provence coal mine (1984-1994).

Table 1: Rock mass mechanical properties (Gaviglio et al., 1996).

Rock type	E (GPa)	ν	ρ (kg/m ³)
Rognacian	1	0.25	2400
Fuvelian	8.4	0.24	2400
Lignite coal	3	0.32	1500
Jurassic	17	0.25	2400

3. GOAF SIMULATION METHODOLOGY

In the current study, the goaf simulation is composed of two different steps. The first step is to estimate the geometry of the goaf (caved zone and fractured zone), the height of the goaf is taken as $32t$ where t (coal seam thickness) = 2.5m (i.e. $h_{\text{caved-zone}}=4t$, Shabanimashcool et al. and $h_{\text{fractured-zone}}=28t$ Peng and Chaing, 1984). The second step is to estimate numerically the mechanical properties within the goaf area. The elastic modulus within the goaf will be calibrated with the convergence between the roof and the floor for only one panel with minimum width (W) 200 m and length (L) varies between 400 m to 1400 m. Then, once the convergence is fulfilled, the model will be calibrated with the in-situ ground surface subsidence for multi-panel with maximum width (W) 1000 m and maximum length (L) 1400 m.

Two different approaches were developed to present the mechanical properties of the goaf (Model 1 and Model 2).

A 3D numerical model of the mine was constructed using the finite difference code FLAC^{3D} (Figure 4). The model contains approximately 2.5 million mesh elements. The mesh density is adjusted to be fine near

to the excavated area and is increased by ratio 1.2 until the model borders. Four different rock types are specified: the coal seam, the Fuvelian, Rognacian with height 400 m and 600 m above the coal seam, and Jurassic limestone beds. The overall dimensions of the model are 4600 m in the x- direction, 6020 m in the y- direction and 2270 m in the vertical direction (z). The top of the model coincides with the ground surface at level $z=0.0$ while the excavated panels lies at depth of 1000 m below the surface. The model boundaries are fixed except the top.

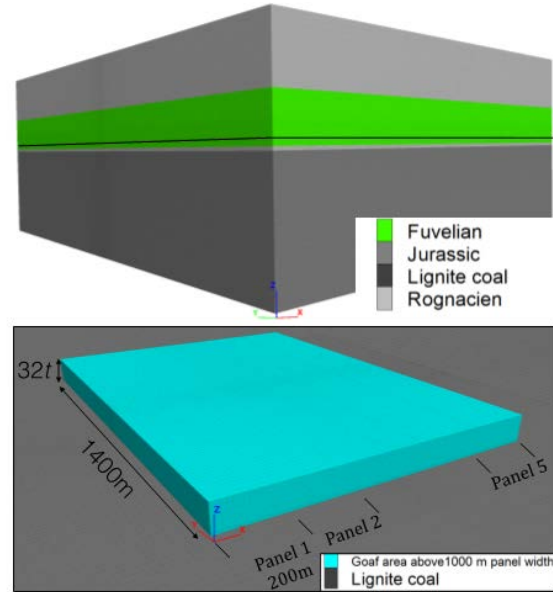


Figure 4: 3D view of the model showing the mining panel and the goaf area.

3.1 Model 1

In this model, we consider that the goaf area is presented by the caved zone and the fractured zone as shown in Fig. 5. The elastic modulus (E) of the fractured zone is assumed to be half of the host rock which is mainly composed of Fuvelian limestone because it is overlying layer above the coal (i.e. $E_{\text{fractured-zone}}= E_{\text{fuvelian}} / 2 = 4.2$ GPa). Nevertheless, iterations were carried out to estimate the caved zone modulus for various length to width ratios ($L/W = 2 - 7$) that satisfy the total convergence between the roof and floor. At first, the elastic modulus of the caved zone is as same as the host rock (i.e. $E_{\text{caved-zone}} = E_{\text{fuvelian}}$) which is called “without goaf”. The last iteration is carried out with $E_{\text{caved-zone}} = 225$ MPa. For all of the performed iteration the Poisson ration has not been changed (i.e. $\nu_{\text{fractured-zone}}= \nu_{\text{caved-zone}}= \nu_{\text{hostrock}}$).

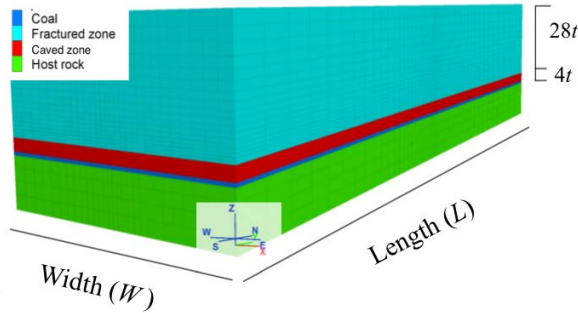


Figure 5: Isometric 3D view of the caved zone and the fractured zone above one panel ($W = 200$ m and $L=1400$ m) (Model 1).

3.2 Model 2

In this model, elastic modulus (E) of the goaf is assumed to vary linearly with the goaf height ($32t$), as shown in Figure 6. The elastic modulus begins from a certain value $E_{immediate-roof}$, which is the value of the elastic modulus of the first few meters in the roof directly above the opening, and increases linearly within the goaf until $E_{hostrock}$ at $32t$ where is the end of the goaf geometry as defined before. $E_{immediate-roof}$ is different than $E_{caved-zone}$ in Model 1, while it is for few meters (not more than 3 m (zone height)), however, $E_{caved-zone}$ has $4t$ height.

Equation (6) was fitted to estimate E_{goaf} at any point within the goaf, by assuming that the Poisson ratio is $\nu_{goaf} = \nu_{hostrock}$ and the direct roof above the excavation has $E_{immediate-roof}$. The only value that could be changed in this model is the $E_{immediate-roof}$, for that, we tried to operate the model with different values of $E_{immediate-roof}$. Four different values have been tried, 600, 450, 225 and 180 MPa respectively. Then, the elastic modulus E_{goaf} could be estimated at any point ($h_g.t$) within the goaf by using equation (6):

$$E_{goaf(h_g.t)} = \left(\frac{E_{hostrock} - E_{immediate-roof}}{x.t} \cdot h_g \cdot t \right) + E_{immediate-roof} \quad (6)$$

where 80, ($32t = 32 \cdot 2.5 = 80$ m), is the maximum height of the goaf that corresponds $E_{goaf(32.t)}$, ($h_g.t$) is the height corresponds to $E_{goaf(h_g.t)}$, h_g ranges between (1 – 32) and t is the coal seam thickness.

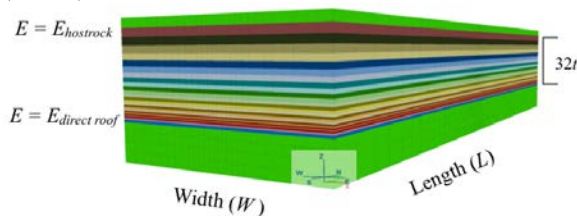


Figure 6: Linear variation of elastic modulus within the goaf area (Model 2).

4. RESULTS AND DISCUSSION

In order to compare the applicability of each of the proposed models each of them were initially calibrated with the total convergence between the roof and floor of the excavated panel that has $W=200$ m and $L=1400$ m. After that, further panels will be exploited with maximum width of 1000 m in order to calibrate the model with the ground surface subsidence. Then, the stress changes due to longwall caving mining will be observed.

4.1 Convergence between roof and floor

In the mine, when a panel is totally mined out, the roof and floor get totally in contact (full closure). However, in the numerical model, due to the hypothesis of elastic behaviour, the convergence between roof and floor might be less than the coal seam thickness. This happens in particular when the stiffness of the roof is equal to that of the host rock (case called “without goaf”).

Figure 7 shows the convergence between roof and floor by using different elastic modulus’ within the caved zone. We can see that the convergence is affected by length to width ratio ($L/W = 2 - 4$), however, for ratio more than 4, the convergence stays nearly constant. Decreasing the elastic modulus (E) of the caved zone in (Model 1) to 225 MPa (i.e. $E_{caved-zone} = 225$ MPa) is sufficient to produce total closure of the coal seam. The convergence remains constant when the modulus is further reducing.

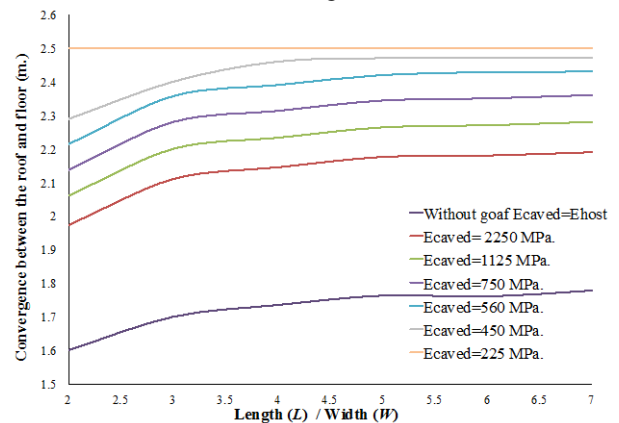


Figure 7: Convergence between roof and floor for different panel lengths with 200 m width (Model 1).

By using Model 2, Figure 8 shows that decreasing the $E_{immediate-roof}$ until 180 MPa is sufficient to produce total convergence between the roof and floor of the panel. For that, in order to get the total touch between the roof and floor (i.e. $convergence = mining\ seam\ thickness (t)$), equation (6) must be written as:

$$E_{goaf(hg,t)} = \left(\frac{E_{hostrack} - 180}{80} \cdot h_g \cdot t \right) + 180 \quad (7)$$

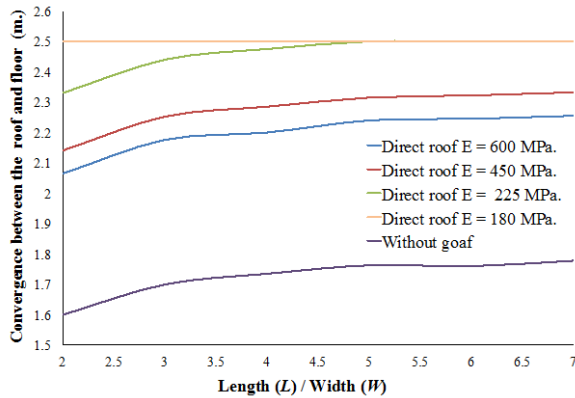


Figure 8: Total convergence between the roof and floor for different panel lengths (Model 2).

Based on the two proposed models, we can find that in case of total convergence after exploitation by using longwall caving, the first damaged few meters in the roof (immediate roof) will have an elastic modulus (E) as:

$$225 \leq E_{immediate-roof} \text{ (MPa)} \leq 180 \quad (8)$$

Although, the two models give approximately a very close range of $E_{immediate-roof}$ and $E_{caved-zone}$ in order to satisfy the total closure of the opining, Model 2 is preferable than Model 1 for simulating the goaf area. Because, the stiffness difference between two adjacent zones should not exceed 10 times, while in Model 1 the difference between the fractured zone and the caved zone is reached to 18 (i.e. $E_{fractured-zone} / E_{caved-zone} = 4200/225 = 18$).

4.2 Ground surface subsidence

One of the very clear observations due to longwall mining is the increasing of the surface subsidence. The panel width has been extended until 1000 m by keeping the maximum length at 1400 m. The proposed model (Model 2) was calibrated with in-situ measurement of the surface subsidence. Figure 9 illustrates the maximum and minimum measured surface subsidence for panel width (W) from 200 m to 1000 m. Model 2 has been applied within various panel widths and the surface subsidence has been measured at the center of the panel. The ground surface subsidence produced by numerical modelling by applying Model 2 is as shown in Figure 9.

The surface subsidence may vary greatly from country to country and from location to location. In case of Provence coalmine, the surface subsidence has been monitored at each excavation step. Figure 9 shows the minimum and the maximum subsidence

values for each panel width to mining depth ratio. For example, for 400 m panel width at 1000 m depth, the (max. subsidence/ t) = 25, so the max. subsidence is $25 \cdot t = 25 \cdot 2.5 = 62.5$ cm.

It is clearly shown that simulating the goaf by using less stiff material has its effect on the surface even with exploitation at very high depth. the influence of the goaf appears on the surface for the panel width (W) / mining depth (H) ratio greater than 0.4. Representing the goaf elastic modulus (E) by using equation (7) gives a rational surface subsidence between the maximum and the minimum in-situ measured subsidence curves. The model without goaf is not able to reproduce even the minimum subsidence curve. The adopted goaf behaviour gives an acceptable subsidence prediction. An improvement can be suggested for large mining areas ($W/H > 1$). In addition, Model 2 will be applied in another future studies to verify its ability to predict the surface subsidence.

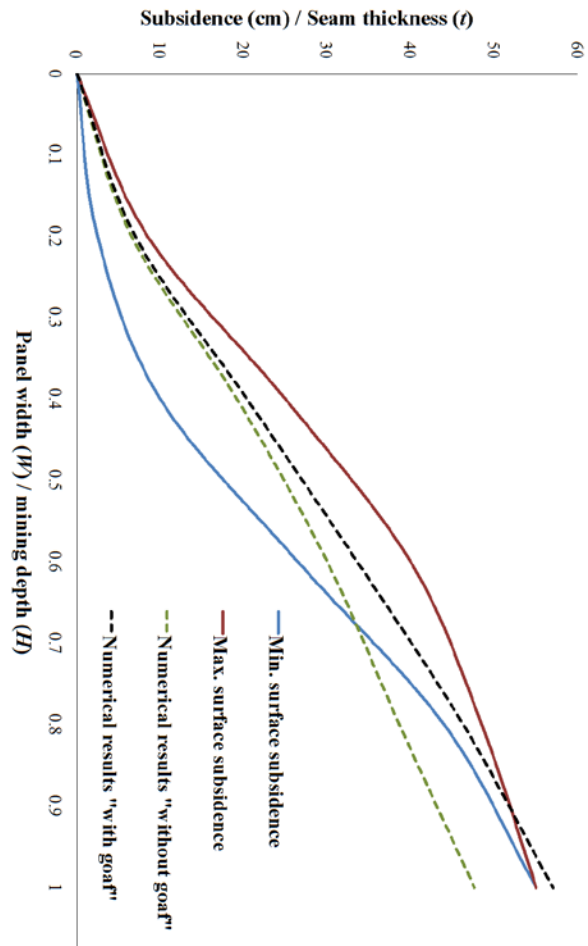


Figure 9: Surface subsidence in case of with and without goaf.

4.3 Stress redistribution

When replacing the goaf area with less stiff material than the host rock, the vertical stress will transfer to the surrounding high stiff materials. The stress distribution due to panel excavation with and without goaf is shown in Figures 10 (a) and (b), respectively. The induced vertical stress within the ribside is 2.5 times the initial one, which is much less than the values given by Wilson (1982b). The induced vertical stress due to goaf has a higher influenced zone horizontally than the case without goaf. Also, the destressing zone is higher in case of the goaf.

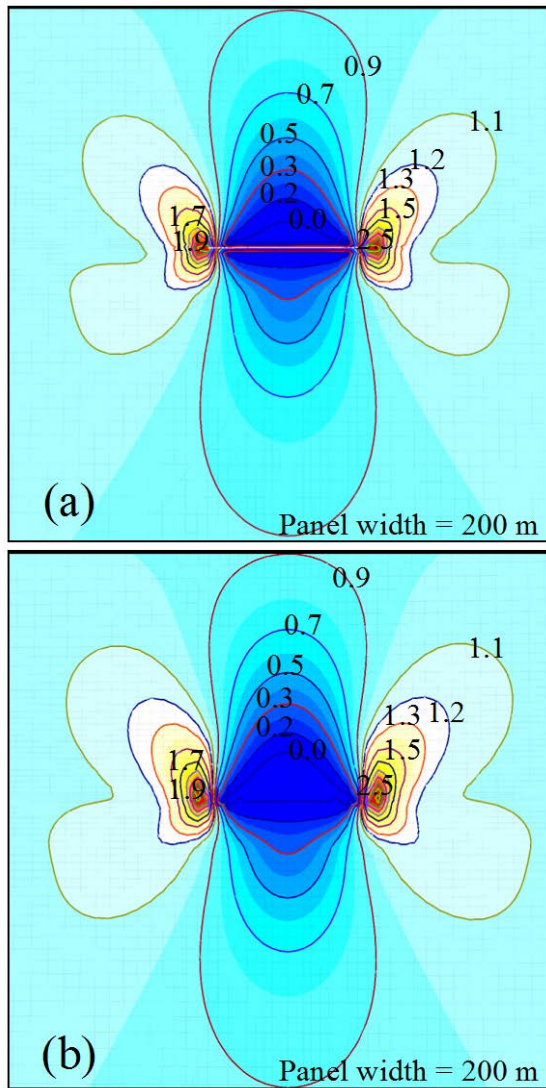


Figure 10: Ratio between induced vertical stress and initial vertical stress (a) without goaf (b) with goaf (Model 2).

As shown in Figure 3, there are rib pillars between two parallel panels. Figure 11 shows the ratio between the induced vertical stress and the initial one in case of excavating two parallel panels with 200 m width and

200 m rib pillar between them. In case of the goaf the influenced zone (horizontally and vertically) within the rib pillar is larger than the case without goaf. By increasing the panel width, the vertical stress will increase at the center of the panel. The induced vertical stress to initial stress ratio is assigned to different panel widths in Figure 12. The results show that when the panel width increases the induced to initial vertical stress ratio increases at the center of the panel. For panel 1000 m width with fully filled mining area, the induced to initial vertical stress ratio is 0.2 at the panel corners until 0.9 at the center without consolidation.

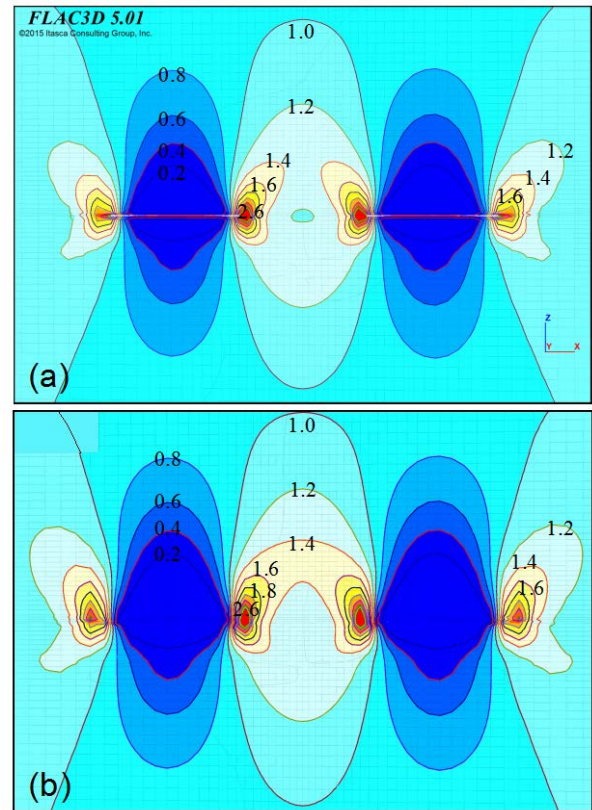


Figure 11: Ratio between induced vertical stress and initial vertical stress within the ribpillar (a) without goaf (b) with goaf (Model 2).

5. CONCLUSION

This research examines the simulation of the goaf area associated with the longwall caving panels of Provence coalmine by using FLAC^{3D}. Two distinct models, Model 1 and Model 2, have been represented to simulate the goaf area after exploitation. Within Model 1 the goaf area is treated as two separated parts (the caved zone and the fractured zone), which have different elastic modulus values.

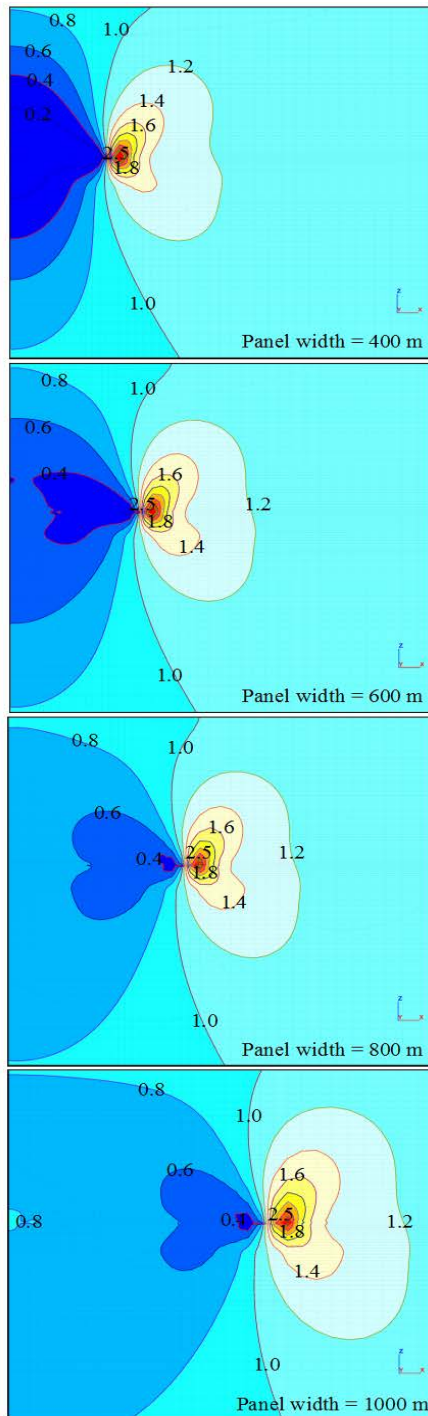


Figure 12: Induced Vertical stress to initial vertical stress distribution within the goaf area for different panel widths.

In Model 2, the goaf area is treated as a one zone with linearly increasing elastic modulus from the direct roof up to the host rock. From the two model, we found that the elastic modulus of the few meters above the panel is ranged between $225 \leq E_{\text{immediate-roof}}$

≤ 180 MPa in order to satisfy the total convergence between roof and floor.

Substituting the goaf area with less stiff material has an effect on the ground surface subsidence for panels whose has width to depth ratio greater than 0.4. Model 2 expresses sufficiently the variation of the elastic modulus within the goaf area. It gave a rational surface subsidence compared with the ‘without goaf’ model. By exploiting a longwall caving panel, the vertical stress within the ribside will increase by 2.5 than the initial value. The vertical stress at the center of a panel whose width to depth ratio is 1 approaches the initial vertical stress value.

6. REFERENCES

- Gaviglio P., 1985. La deformation cassante dans les calcaires Fuvéliens du basin de l’arc (Provence). PhD thesis. University of Provence, Marseille, France.
- Gaviglio P, Bigarre P, Baroudi H, Piguet J.P and Monteau R. (1996). Measurements of natural stresses in a Provence mine (Southern France). *Journal Engineering Geology*. Volume 44, pp. 77-92.
- Pappas DM and Mark C., 1993. Behaviour of simulated longwall gob material. Report of investigation no. 9458, US Department of the Interior, Bureau of Mines, 39 p.
- Peng S.S. and Chaing H.S. (1984) Longwall Mining. John Wiley & Sons Inc., New York; pp. 17-73
- Salamon MDG. (1990). Mechanism of caving in longwall mining. In: Hustrulid W, Johnson G, editors. *Proceedings of the 31st US rock mechanical symposium*, Golden, Colorado. Rotterdam: Balkema, pp. 161–68.
- Shabanimashcool, M. and Charlie, C.L. (2012) Numerical modelling of longwall mining and stability analysis of the gates in a coal mine. *International Journal of Rock Mechanics and Mining Science*. Volume 51, pp. 24–34.
- Sheorey P. R. (1993) Design of coal pillar arrays and chain pillars. *Comprehension Rock Engineering*, Vol. 2. Pergamon Press, Oxford.
- Wilson A. H. (1982). Pillar stability in longwall mining. *State of the Art of Ground Control in Longwall Mining and Mining Science*, Y. P. Chugh and M. Karmis (eds.), SME, New York; pp. 85-95.
- Wilson A.H., 1980. The stability of underground workings in the soft rocks of coal measures. Unpublished Ph.D Thesis, Univ. Nottingham.
- Yavuz H. (2004) An estimation method for cover pressure re-establishment distance and pressure distribution in the goaf of longwall coal mines. *International Journal of Rock Mechanics and Mining Science*. Volume 41, pp. 193–205.